X-ray Scattering Study of the Melting Transition of a CCl4 Monolayer on Graphite

P. Aranda, T. Ceva, B. Croset, N. Dupont-Pavlovsky, M. Abdelmoula

X-ray Scattering Study of the Melting Transition of a CCl_4 Monolayer on Graphite

P. Aranda ([1]), T. Ceva ([1]), B. Croset ([1,*]), N. Dupont-Pavlovsky ([2]) and M. Abdelmoula ([3])

([1]) Groupe de Physique des Solides (**), Universités Paris 6 et Paris 7, Tour 23-13, 2 place Jussieu, 75251 Paris Cedex 05, France
([2]) Laboratoire de Chimie du Solide Minéral (***), Université Nancy 1, boulevard des Aiguillettes, B.P. 239, 54506 Vandœuvre les Nancy, France
([3]) Laboratoire M. Letort, 45 rue de Vandœuvre, 54600 Villers les Nancy, France

(Received 10 January 1996, received in final form 25 March 1996, accepted 9 April 1996)

PACS.68.35.Rh – Phase transitions and critical phenomena
PACS.64.70.Dv – Solid-liquid transitions
PACS.68.45.Da – Adsorption and desorption kinetics; evaporation and condensation

Abstract. — We have performed an extensive X-ray scattering study of 0.85 monolayer of carbon tetrachloride adsorbed on graphite with a rotating anode X-ray generator. By using a position sensitive detector, we were able to study simultaneously two diffraction peaks during the whole melting transition. A measure of the Debye-Waller correlation function coefficient, η_{Q_B}, based on peak broadening was performed for the two peaks in the solid regime. The proportionality law between these two coefficients has been verified, with a fairly good agreement and it confirms the quasi-long-range order in the solid. At melting, the coefficient η_{Q_B} for the first peak is equal to 0.23, a value compatible with previous experimental work and standard theory. The intensities of the diffraction peaks exhibit variations with η_{Q_B} and coherence length which are in agreement with theoretical predictions in both solid and liquid regimes.

1. Introduction

Volumetric and X-ray scattering studies of the carbon tetrachloride (CCl_4) adsorption on the basal plane of graphite have been performed by Abdelmoula *et al.* [1]. Using a position sensitive detector with a large angular domain, these authors were able to follow the modifications of two Bragg peaks (indexed (10) and (11)) simultaneously. The CCl_4 monolayer melting was qualitatively shown to be continuous. This result was in contradiction with conclusions drawn by Stephens *et al.* [2] in their study of the phase diagram of CCl_4 on graphite up to two layers. Prior to our work, Heiney *et al.* [3] and Nielsen *et al.* [4] studied the melting of Xe and Ar on graphite using synchrotron radiation or a rotating-anode X-ray generator. Although they mainly considered a single Bragg peak, these authors also concluded that melting of such monolayers is a continuous transition.

(*) Author for correspondence: (e-mail: croset@gps.jussieu.fr)
(**) *URA CNRS 17*
(***) URA CNRS 158

Two-dimensional (2D) systems which undergo a continuous transition can be studied in the frame of the 2D melting theory elaborated by Kosterlitz, Thouless, Halperin, Nelson and Young (KTHNY) [5–7]. Halperin and Nelson [6] gave suggestions to check their theory by means of X-ray scattering: their paper proposes to study the behaviour of the diffraction peak shape in the solid before melting and the behaviour of the intensity of the diffraction peak in the liquid.

Although the KTHNY theory is already several years old and an important experimental and numerical work has been devoted to it [8–17], the 2D melting remains a topical subject [18]. The study by Abdelmoula *et al.* of CCl_4 adsorbed on graphite prompted us to choose the same system in our study of the 2D melting in spite of the absence of the (20) Bragg reflection peak shown by X-ray and neutron scattering [1, 19]. When looking for an explanation for this (20) peak absence, both the high symmetry of the CCl_4 molecule and the hexagonal cell must be kept in mind. First, the ratio of the Bragg vectors for the (20) and (11) peaks, $Q_B(20)/Q_B(11)$, being much lower than $Q_B(11)/Q_B(10)$, an abnormal static Debye-Waller factor leading to the disappearance of (20) peak should lead to the disappearance of (11) peak as well. Second, the intramolecular distance and the intermolecular distance being of the same order of magnitude, a molecular form factor, leading to the (20) extinction, should also lead to a quite low value of the (11) peak intensity in a Bravais lattice case. Third, a complex cell, multiple of the hexagonal cell, may lead to a special extinction law for the (20) peak but, in counter part, it should lead to the appearance of additional peaks of non integer indices; there is no experimental evidence of such peaks in the whole studied Q-domain. This lack of easy explanation to the (20) peak absence compels us to assume, without proof, that it has no consequence on the physics of melting. Our study is different, in many respects, from the study performed by Abdelmoula *et al.* First, the exploration of the temperature domain is more systematic. Second, the analysis method of the experimental spectra is different. Finally, the experimental environment has been modified: we use a rotating-anode X-ray generator; the scattering is done in a transmission geometry instead of the reflection geometry used by Abdelmoula *et al.*; in order to facilitate the analysis of the spectra and the background determination, the angular domain has been extended toward small angles.

In this paper, we present a detailed quantitative X-ray investigation of the continuous liquid-solid transition undergone by the CCl_4 monolayer adsorbed on graphite. To our knowledge, this is the first study of bidimensionnal melting of a physisorbed layer performed using two diffraction peaks. In order to estimate the exponent η_{Q_B} of the Debye-Waller correlation function from the relative broadening of the diffraction peaks, we use the method that we proposed in a recent paper [20]. In Section 2, we present the experimental method. In Section 3, the primary results obtained are shown and discussed. In Section 4, the data reduction is explained, namely the method of η_{Q_B} determination. In Section 5, we discuss the η_{Q_B} values, the coherence lengths and the intensities for the two diffraction peaks.

2. Experimental Details

The substrate was Le Carbone Lorraine-Papyex exfoliated graphite. It was outgassed at 800 °C and mounted in the sample cell under N_2 atmosphere. The sample size was $12 \times 12 \times 1.2\ mm^3$. The sample cell, built with copper and having Mylar windows, was installed at the extremity of an Air Products Displex cryogenerator. The commensurate-incommensurate transition of krypton studied by X-ray scattering was used in order to determine the amount of adsorbed gas corresponding to a monolayer. The krypton amount at the completion of the commensurate $\sqrt{3} \times \sqrt{3}$ structure was measured by monitoring the pressure on the sample during the transition, knowing the introduced amount of gas in the sample cell. In order to determine the crystal characteristics of the Papyex sample (coherence length, mosaicity), the (10) Bragg peak

of commensurate adsorbed krypton was used as a reference. The (10) Bragg peak of krypton was fitted quite well by a Warren type model with a powder proportion equal to 5% and a half width at half maximum (HWHM) mosaicity of 17.6°, using as a line shape for the rows the convolution of a Lorentzian (HWHM of 0.017 $Å^{-1}$) with a Gaussian (HWHM of 0.009 $Å^{-1}$).

The CCl_4 (99.8% purity) was obtained from Prolabo. Before each experiment, it was purified by pumping on the condensed phase at 193 K (dry-ice temperature) inside the volumetric apparatus. Because of the presence of Cl atoms, CCl_4 has a large X-ray scattering cross-section. The molecule is a quite spherical molecule and this gas obeys the law of corresponding states, *i.e.*, the $T_c(2D)/T_c(3D)$ ratio is similar to those of noble gases. The 2D solid structure exhibits two diffraction peaks. The ratio of their positions is equal to $\sqrt{3}$ and they can be indexed as the (10) and the (11) peaks of an hexagonal close-packed structure. This structure is very incommensurate since its parameter differs by 8% from the nearest commensurate structure $\sqrt{7} \times \sqrt{7}$. This incommensurate hexagonal case is the subject of seminal theoretical papers on continuous 2D melting [5–7]. The utilisation of a detector with a large angular domain allows us to observe the two diffraction peaks for the same position of the detector. Because these two peaks are well separated from those of the substrate and in order to protect the detector from carbonisation, we placed on it a Pb mask to shield the very intense (002) graphite peak.

A Rigaku 12-kW rotating-anode X-ray generator operating at 11.4 kW was used as an X-ray source. The 2-axis diffractometer was equipped with a graphite primary monochromator selecting the CuK_α radiation ($\lambda_{K_\alpha} = 1.5418$ $Å^{-1}$). The position-sensitive linear detector was devised and built by M. Gabriel from the European Molecular Biology Laboratory in Grenoble (France); it used a gas circulation of a 70% Ar, 30% CO_2 mixture. The Papyex sample was in a focusing transmission geometry; this allows coincidence between the focusing orientation and the orientation of the preferential c-axis direction.

The sample temperature was measured with a stability of ±0.05 K over a 24 h period with an absolute accuracy of 0.1 K. A temperature scanning was done from low to high temperatures and from high to low temperatures. The equilibrium pressure on the sample was low enough to assume a constant adsorbed amount during the phase transition and the whole scanning. For each experiment, the gas was introduced in contact with the sample at 240 K, in order to check the adsorption equilibrium by means of pressure measurements. Lower temperatures were then slowly reached in order to avoid gas condensation on the cell walls.

3. Determination of the Order of the Solid-Liquid Transition

Figure 1 shows some of the spectra obtained between 40 K and 240 K with 0.85 CCl_4 monolayer adsorbed on graphite. The data acquisition time was four hours for each spectrum. A background scattering intensity from the bare substrate has been subtracted to the spectra measurements with 0.85 monolayer. The temperature scanning showed in Figure 1 was performed from high temperatures to low temperatures. The same results are obtained with the reverse temperature scanning. By using the simultaneous scattering of two diffraction peaks, a determination of the order of the transition can be done with a simple qualitative analysis. For each peak, its vanishing is preceded by its broadening and we can notice that the (11) Bragg peak broadens and vanishes 10 K before the (10) Bragg peak. For instance, as clearly shown by the detailed Figure 2c, the 197 K-spectrum has at the same time a solid and sharp (10) Bragg peak and a vanishing (11) Bragg peak.

It may be tempting to interpret the intermediary shape of each peak as the linear combination of a liquid and a solid peak shape and we think that the use of only the first peak during their preliminary study of CCl_4 melting has led Stephens *et al.* to identify the process as a first order

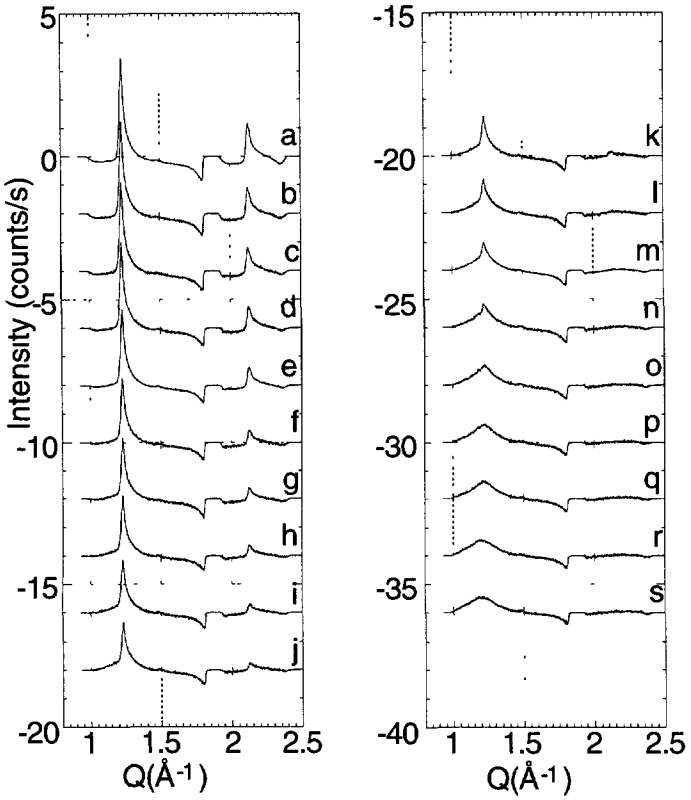

Fig. 1. — Diffraction profiles of 0.85 monolayer CCl_4 films adsorbed on graphite (a, 40 K; b, 132 K; c, 150 K; d, 160 K; e, 170 K; f, 179 K; g, 182 K; h, 185 K; i, 188 K; j, 191 K; k, 194 K; l, 197 K; m, 200 K; n, 203 K; o, 206 K; p, 209 K; q, 210 K; r, 220 K; s, 230 K).

transition. Nevertheless as is clearly shown in Figure 2, at any intermediary temperature (*e.g.* 170 K Fig. 2a, 182 K Fig. 2b, 197 K Fig. 2c), a simultaneous good description of both Bragg peaks is impossible. A good agreement on one peak leads to a bad agreement on the other peak. This impossibility to describe correctly intermediary spectra by linear combination of a liquid and a solid spectra is mainly due to the fact that these reference spectra must be chosen at very different temperatures (230 K and 132 K) because of the very large amplitude of the transition domain. Strictly speaking, our study being done at constant coverage and varying temperature, we have no access to the reference spectra usable for such linear combination and a very rapid variation of the solid and liquid spectra with temperature may explain our difficulty in obtaining a good agreement between intermediary spectra and linear combination. But such a rapid variation of the coexisting liquid and solid seems incompatible with a large amplitude of the transition domain. We conclude that the melting is mainly continuous although we cannot exclude a residual first order discontinuity. In the following, we will try to explore the experimental characteristics of such a continuous transition. We will first study the broadening of the peaks by fitting the experimental spectra with calculated profiles.

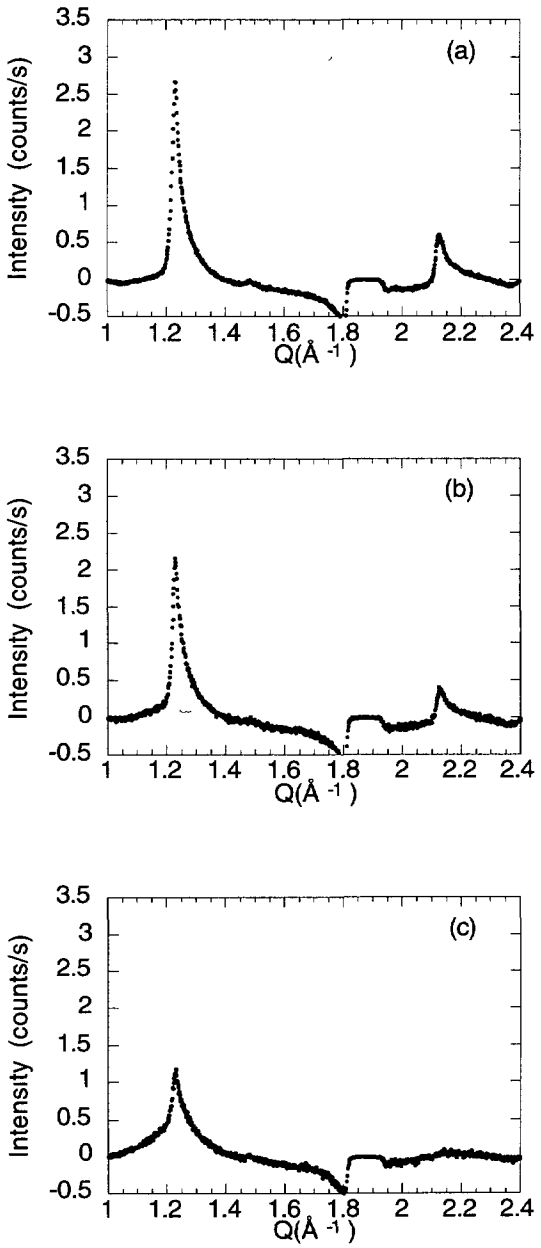

Fig. 2. — Diffraction profiles of 0.85 monolayer CCl_4 films adsorbed on graphite at intermediary temperatures (a, 170 K; b, 182 K; c, 197 K).

4. Data Reduction and η_{Q_B} Measure

Because of the necessity of a Warren-transform [21], *i.e.*, the calculation of the diffracted intensity taking into account a summation on the crystallites orientations, it is impossible to obtain straightaway the parameters accounting for the scattering cross section $S(Q)$. Therefore

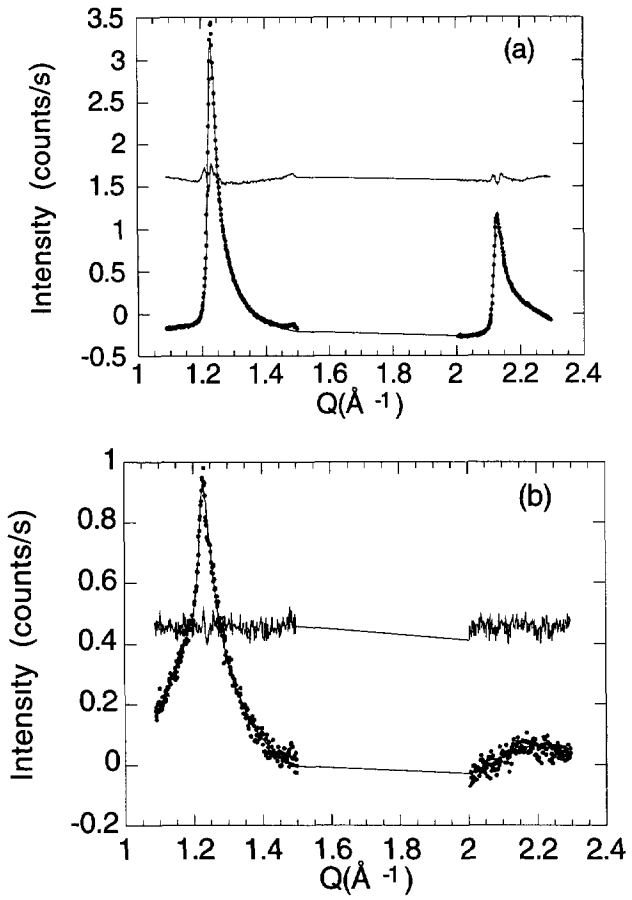

Fig. 3. — 0.85 CCl_4 monolayer diffraction profiles at 40 K (a) and at 197 K (b). Solid lines are double Lorentzian fits for each peak and difference between observed and calculated intensity.

the position, *i.e.* the Bragg vector Q_B, the width κ and the intensity I characterising each peak of $S(Q)$ have to be determined by computing the profile $S(Q)$ for which the Warren-transform allows the best fit to the experimental spectrum.

Let us note η_{Q_B}, the exponent describing the decay in direct space of the Debye-Waller correlation function [6], $\langle \exp\{i\mathbf{Q}_B(\mathbf{U}(\mathbf{R}) - \mathbf{U}(\mathbf{0}))\}\rangle$ (with $\mathbf{U}(\mathbf{R})$ being the displacement of the $\mathbf{R}$-atom and the brackets standing for the thermal average). In a previous paper [20], two of the authors have proposed a η_{Q_B} measure which is quasi-insensitive to the $S(Q)$ detailed shape but needs a precise determination of its half width at half maximum. In order to use all the statistical information, it is essential to determine this width by measuring it on the $S(Q)$ profile obtained by a least-squares fit of the diffracted intensity.

By choosing for $S(Q)$ the sum of two variable-width Lorentzians convoluted with a Gaussian of fixed width, we obtain, at each temperature and for the two peaks, satisfactory agreements as shown in Figure 3. The Gaussian width has been determined to be equal to 0.009 $Å^{-1}$ using the krypton (10) commensurate Bragg peak. Such a Gaussian convoluted with a unique Lorentzian allows a very good fit of each of the two peaks at 40 K.

Our method for measuring η_{Q_B} is very different from that used by Heiney *et al.* [3] who directly compared the profile proposed by Dutta and Sinha [22] to the experimental profile. In the method employed by Heiney *et al.*, the determination of two independent parameters, κ_0, the inverse of the coherence length and η_{Q_B} from a least-squares fit, requires a precise knowledge of the behaviour of $S(Q)$ at high modulus of $\mathbf{q} = \mathbf{Q} - \mathbf{Q}_B$, but this precise knowledge is experimentally difficult to obtain. In a recent and very precise experiment, Nuttall *et al.* [18] noticed that, despite the use of a monocrystalline substrate and of synchrotron radiation, such a procedure cannot give access to a physically significant value of η_{Q_B} but only to its variation.

In order to test our method for measuring η_{Q_B}, we performed this measure using not only the broadening at half maximum but also the broadenings at a quarter, at three-fourths and at four-fifths of the maximum measured on the $S(Q)$ obtained for each peak and at each temperature.

Following Aranda *et al.* [20], at half maximum, a good measure of η_{Q_B} is the function $g_{1/2}(\Delta'_{1/2})$ defined as:

$$g_{1/2}(\Delta'_{1/2}) = \frac{-2\ln 2}{\ln\left(1 + (\Delta'_{1/2})^2\right) + \ln 2} + 1$$

where $\Delta'_{1/2}$ is the relative broadening, $\Delta'_{1/2} = \kappa(\eta_{Q_B}(T))/\kappa(\eta_{Q_B}(0))$, with κ = half width at half maximum on the fitting profiles.

Other measures of η_{Q_B} may be obtain calculating broadening using the peak width at the m-th of the maximum:

$$g_m(\Delta'_m) = \frac{2\ln(m)}{\ln\left(1 + (1-m)\left((\Delta'_m)^2\right)/m\right) + \ln(m)} + 1.$$

In Figure 4, the widths at a quarter, at half, at three-fourths and at four-fifths of the maximum for each peak are plotted as a function of temperature. Comparing these curves, it is obvious that the (11) Bragg peak apparently broadens 10 K before the (10) Bragg peak, regardless of the height considered.

In Figure 5 the values of η_{Q_B} determined using these different widths are compared to the determinations of η_{Q_B} using HWHM. The determinations of η_{Q_B} performed using the peak widths at half, three-fours and four-fifths of the maximum lead to the same values and, therefore, we chose the determination of η_{Q_B} using HWHM as a good measure of η_{Q_B}. The determination of η_{Q_B} at a quarter of the maximum begins to be different from the common behaviour when η_{Q_B} is equal to 0.2. This discrepancy is possibly due to the sensitivity of the high q tail to details of the diffracting sample for large values of η_{Q_B}, as pointed by Aranda *et al.*

5. Data Analysis

Our temperature study scans the solid domain, the melting transition and the liquid domain. In the solid domain, a scattering spectrum was performed at 40 K, then every 3 K between 132 K and 150 K and every 2 K between 150 K and 172 K. In the melting domain, between 172 K and 210 K, the choice of step is 1.5 K and in the liquid domain, 230 K is reached in steps of 10 K.

5.1. PEAK POSITION. — Figure 6 shows the dependence on temperature of the ratio between (11) Bragg peak position and (10) Bragg peak position. At 40 K, (10) and (11) Bragg peak positions are 1.221 $Å^{-1}$ and 2.122 $Å^{-1}$ and, as expected for an hexagonal structure, the ratio

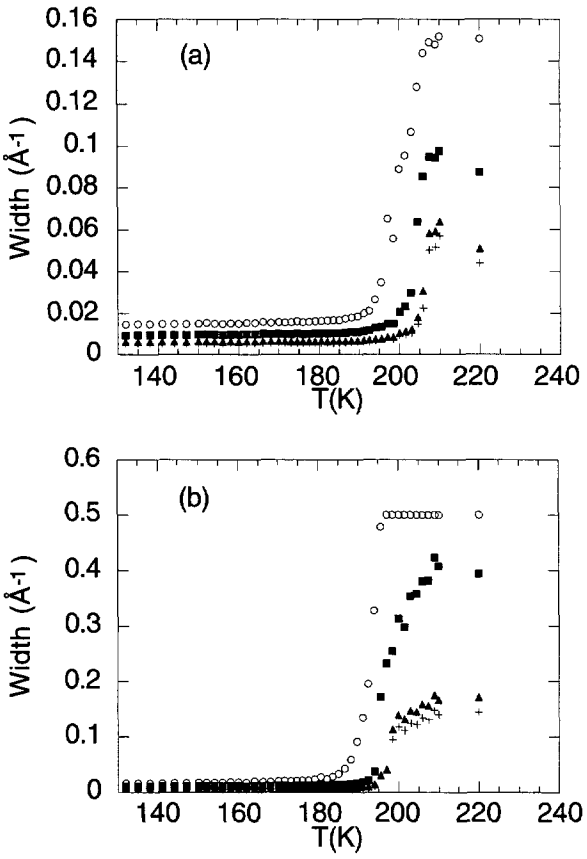

Fig. 4. — Peaks widths at a quarter (○), half (▲), three-fourths (■) and four-fifths (+) of the maximum of the peak intensity *vs.* temperature. ((10) peak curves (a), (11) peak curves (b)).

is equal to $\sqrt{3}$. Up to 197 K, the difference between $\sqrt{3}$ and the ratio of the positions is lower than 0.3%. Moreover, this difference is less than 5% up to 210 K, and it should be noticed that, at this temperature, the diffraction peaks are quite broad with a width representing more than 10% of their position. All these results clearly show that the liquid has kept in memory the solid quasi-long-range order. Such a result is expected in a KTHNY melting description, as well as in any model describing the liquid as a solid with short coherence lengths, but is unusual for ordinary three-dimensional liquids.

5.2. η_{Q_B} COEFFICIENT. — Figure 7 and Table I show the variation of η_{Q_B} for both the (10) and the (11) Bragg peaks. As explained in Section 4, we used the relative broadening to measure η_{Q_B}. This procedure requires the knowledge of the peak width at very low η_{Q_B}, and we assumed that the 40 K peaks correspond to such low values. As noticed in Aranda *et al.* [20], it is difficult to determine the nature of the order using the precise shape of the peaks but a good test of the quasi-long-range order should be the verification, in the case of an hexagonal structure, of the simple law: $\eta_{11} = 3\eta_{10}$. The simultaneous observation of two peaks allowed this verification. In Figure 8, the η_{11} dependence on η_{10} is shown. The expected proportional

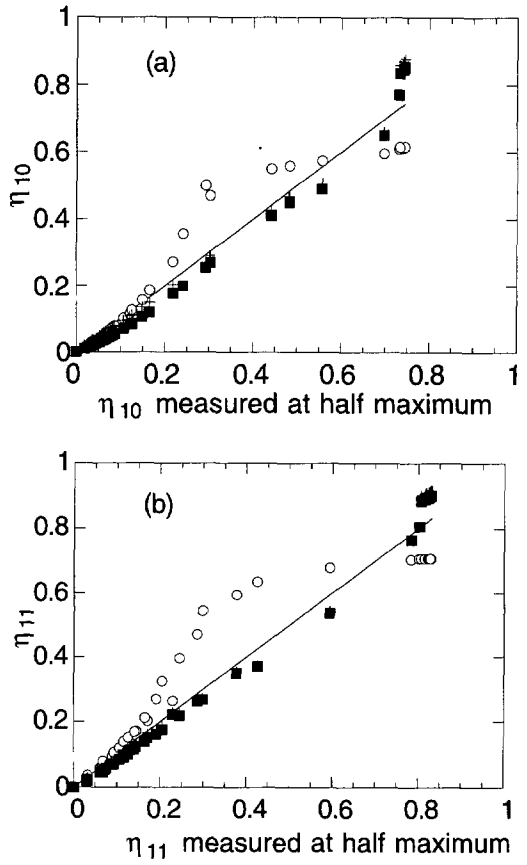

Fig. 5. — Comparison of the measures of η_{Q_B} at a quarter (○), half (—), three-fourths (■) and four-fifths (+) of the maximum of the peak intensity ((10) peak curves (a), (11) peak curves (b)).

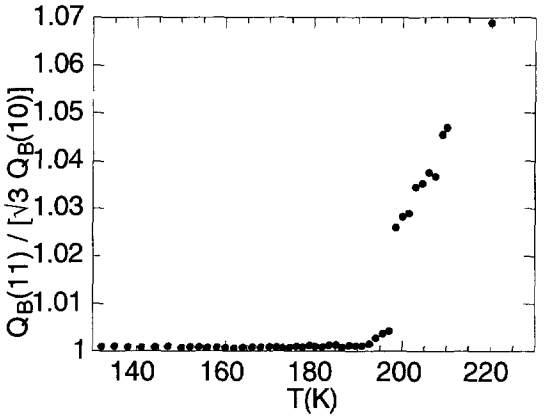

Fig. 6. — Ratio $Q_B(11)/[\sqrt{3}Q_B(10)]$ *vs.* temperature.

Table I. — *Width parameters obtained by least-square fits of diffraction data by double Lorentzian line shape. T is the temperature, $\kappa(hk)$ is the HWHM of the (hk) peak, $\Delta'_{1/2}(hk)$ is the relative broadening at half maximum.*

T (K)	κ (10) (Å^{-1})	$\Delta'_{1/2}(10)$	η_{10}	κ (11) (Å^{-1})	$\Delta'_{1/2}(11)$	η_{11}
40.0	0.00916	1.000	0.000	0.00982	1.000	0.000
132.0	0.00940	1.026	0.019	0.01028	1.047	0.033
135.0	0.00949	1.036	0.025	0.01024	1.043	0.030
138.0	0.00952	1.039	0.028	0.01025	1.044	0.031
141.0	0.00957	1.045	0.031	0.01028	1.047	0.033
144.0	0.00951	1.038	0.027	0.01071	1.091	0.061
147.0	0.00957	1.045	0.031	0.01079	1.099	0.066
150.0	0.00966	1.055	0.038	0.01114	1.134	0.088
152.0	0.00988	1.079	0.054	0.01114	1.134	0.088
154.0	0.00968	1.057	0.039	0.01093	1.113	0.075
156.0	0.00953	1.040	0.028	0.01088	1.108	0.072
158.0	0.00976	1.066	0.045	0.01161	1.182	0.116
160.0	0.00962	1.050	0.035	0.01117	1.138	0.090
162.0	0.00989	1.080	0.054	0.01082	1.102	0.068
164.0	0.00987	1.077	0.053	0.01190	1.212	0.132
166.0	0.01009	1.102	0.068	0.01123	1.144	0.094
168.0	0.00988	1.079	0.054	0.01146	1.167	0.107
170.0	0.01001	1.093	0.063	0.01173	1.194	0.122
171.5	0.00996	1.087	0.059	0.01179	1.201	0.126
173.0	0.00996	1.087	0.059	0.01164	1.185	0.117
174.5	0.01022	1.116	0.077	0.01181	1.203	0.127
176.0	0.00997	1.088	0.060	0.01216	1.238	0.146
177.5	0.01006	1.098	0.066	0.01208	1.230	0.141
177.5	0.01006	1.098	0.066	0.01208	1.230	0.141
179.0	0.01018	1.111	0.074	0.01266	1.289	0.171
180.5	0.01029	1.123	0.082	0.01397	1.423	0.230
182.0	0.01024	1.118	0.078	0.01254	1.277	0.165
183.5	0.01033	1.128	0.084	0.01310	1.334	0.192
185.0	0.01039	1.134	0.088	0.01341	1.366	0.206
186.5	0.01070	1.168	0.108	0.01436	1.462	0.245
188.0	0.01094	1.194	0.122	0.01550	1.578	0.287
189.5	0.01101	1.202	0.127	0.01589	1.618	0.300
191.0	0.01142	1.247	0.150	0.01876	1.910	0.378
192.5	0.01171	1.278	0.166	0.02106	2.145	0.426
194.0	0.01278	1.395	0.218	0.03730	3.798	0.596
195.5	0.01332	1.454	0.242	0.17167	17.482	0.784
197.0	0.01466	1.600	0.294	0.23193	23.618	0.802
198.5	0.01494	1.631	0.304	0.25467	25.934	0.808
200.0	0.02048	2.236	0.442	0.31289	31.863	0.818
201.5	0.02300	2.511	0.483	0.29712	30.257	0.816
203.0	0.02958	3.229	0.557	0.35328	35.976	0.824
204.5	0.06365	6.949	0.698	0.35721	36.376	0.824
206.0	0.08525	9.307	0.732	0.38063	38.761	0.827
207.5	0.09479	10.348	0.742	0.38172	38.872	0.827
209.0	0.09446	10.312	0.742	0.42249	43.023	0.831
210.0	0.09753	10.647	0.745	0.40761	41.508	0.830
220.0	0.08744	9.546	0.734	0.39374	40.096	0.828

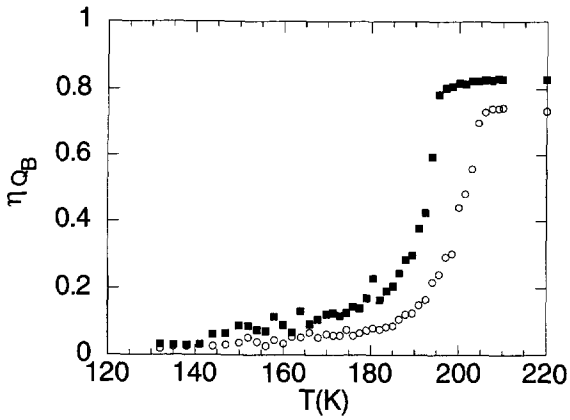

Fig. 7. — η_{10} (○) and η_{11} (■) *vs.* temperature.

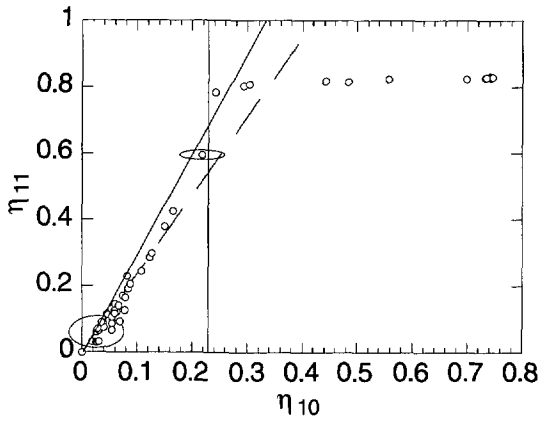

Fig. 8. — η_{11} *vs.* η_{10} (vertical line: limit of the linear behaviour; dashed line: $\eta_{11} = 2.4\ \eta_{10}$; solid line: $\eta_{11} = 3\ \eta_{10}$; typical errors ellipses at low and high η_{Q_B} calculated with a relative error on the peak width equal to 5%).

behaviour is verified up to $\eta_{10} = 0.23 \pm 0.04$. By unweighted least-square fits of the linear zone, *i.e.*, for η_{10} values lower than 0.23, the proportionality coefficient is determined to be equal to 2.4 ± 0.2. The typical error bars of η_{11} and η_{10} are plotted. They may seem quite important but these high uncertainties, particularly for low η_{Q_B}, are due to the difficulty to measure the small relative broadenings and to the logarithmic dependence of η_{Q_B} on this broadening. It is interesting to notice that:

- first, the proportional law with a coefficient equal to 3 is compatible with the data, because the solid line representing this law cuts all the error bars of the experimental points;
- second, the numerous measurements at low η_{Q_B} are mainly responsible for the 2.4 determination of this coefficient in least-squares procedure;
- third, at low η_{10} correspond low η_{11}, *i.e.* the straight line obtained by linear regression intercepts the origin.

We interpret these results as follows:

- $T = 194$ K, corresponding to $\eta_{10} = 0.23$, which is the end of the linear behaviour, is the melting temperature. This temperature is the same as that determined by Abdelmoula *et al.* [1] from a qualitative interpretation of their spectra.
- In the solid domain, below 194 K, the simple law $\eta_{11} = 2.4\ \eta_{10}$ is verified from low values of η_{10} to high values of η_{10}, *i.e.*, from cold solid to melting. The proportionality coefficient, 2.4, is close to 3, the expected coefficient for an hexagonal structure with isotropic sound velocity, and to 2, the value measured by Heiney *et al.* [3] in the case of xenon adsorbed on graphite. This proportionality is a good verification of the quasi-long-range nature of the order in the solid.
- In the liquid or hexatic domain, *i.e.* above 194 K, the coherence length is not constant and the measures of η_{Q_B} built on relative broadening are no longer valid. As a matter of fact, the use of a powder sample does not allow the experimental differentiation between these two phases.

Nevertheless, this interpretation corresponding to the KTHNY theory is not flawless:

- First, the absence of the (20) peak prevents the verification of another simple law: $\eta_{20} = 4\eta_{10}$.
- Second, with the powder diffraction method used, we cannot measure values of η_{Q_B} larger than 1. The lack of linearity for values of η_{10} larger than 0.23 may come from this limitation on η_{11} values. But it must be pointed out that 0.23, the value of η_{10} at melting, is nearly compatible with the predictions made by HNY who proposed a value between 0.25 and 0.33. In their study of the melting transition of a xenon monolayer, Heiney *et al.* have found an interval $0.27 < \eta_{10}(\text{melting}) < 0.42$. Later, Dimon *et al.* [23] found an interval $0.24 < \eta_{10}(\text{melting}) < 0.35$ for the same system. Both these results are consistent with ours and are claimed by the authors, to be consistent with HNY predictions.

Our interpretation becomes more convincing when we study the intensity. Yet, in order to analyse the intensity variation, we first have to study the coherence length in the liquid above 194 K.

5.3. Coherence Length in the Liquid. — The experimental spectra clearly show that the (11) Bragg peak is broader than the (10) Bragg peak in this temperature range. This fact is in contradiction with the direct interpretation of the (10) Bragg peak width as the inverse of a coherence length as done by Heiney *et al.* [3] and Nielsen *et al.* [4], since such an interpretation should lead to the same width for both peaks.

This interpretation is due to the fact that the Debye-Waller correlation function proposed for the liquid (and the hexatic phase) by Halperin and Nelson is an exponential characterised by a coherence length L which represents the mean distance between isolated dislocations. This exponential dependence of the Debye-Waller correlation function and the variation of L with temperature represents the main characteristic of the order in the liquid. Nevertheless, when used to calculate diffraction peak profiles, this too simple expression leads to unphysical results. It not only predicts an equal width for each peak but also a discontinuity in the peak shape at the transition. As shown by previous works and as discussed in 5.2, thermal vibrations in the solid phase broaden diffraction peaks because of their power law contribution to the Debye-Waller correlation function. The absence of such a power law variation in the liquid Debye-Waller correlation function will lead to a discontinuity of the profile shape, by producing at the transition a narrowing of the profile. Nevertheless compression modes are still present in the liquid phase and the summation of their contributions exhibits the usual

infrared divergence and therefore should lead to a power law contribution to the Debye-Waller correlation function.

Finally, the usual correlation function used in scattering techniques to describe finite size effects in perfect solids (*i.e.* at zero temperature) is an exponential and leads to Lorentzian profiles for the diffraction peaks in powder spectra. Consequently, for a given value of η_{Q_B}, the diffraction peak profile of a solid with a finite size and the diffraction peak profile of a liquid with a fixed coherence length are identical: substituting the coherence length to the finite size in the exponential part of the Debye-Waller correlation function is sufficient. In other words, the liquid phase as described by Nelson and Halperin must be understood as a microcrystalline phase with quasi-long-range order.

Nevertheless, the variation of the peak widths are due to different mechanisms in the solid and in the liquid. In the solid, η_{Q_B} varies as long as the average distance between the elements of a dislocation pair increases and the coherence length is constant because it is due to the finite size of the crystallites; on the other hand, in the liquid, η_{Q_B} is constant and is equal to $\eta^*_{Q_B}$, as indicated by HNY, and the coherence length, defined as the characteristic distance between isolated dislocations, varies.

As we have shown in our previous paper [20] and as noticed in previous experimental works, it is quite difficult to distinguish a true Lorentzian profile from a "quasi-long-range order" profile. But, as noticed in Section 4 and in the preceding discussion, the "quasi-long-range order" broadens the peaks, and in order to have access to the liquid coherence length, it is necessary to invert the expression used for the measure of η_{Q_B} in Section 4:

$$L_{\text{eff}} = \frac{B}{\kappa} = \frac{\sqrt{2^{(1+\eta^*_{Q_B})/(1-\eta^*_{Q_B})} - 1}}{\kappa}$$

Even though $\eta^*_{Q_B}$ is constant for each peak in the liquid phase, it varies from peak to peak since it is proportional to the square of the Bragg vector.

From the previous equation, for the 10 peak $\eta^*_{10} = 0.23$, $L_{\text{eff}} = 1.4/\kappa(10)$ and for the 11 peak $\eta^*_{11} = 0.69$, $L_{\text{eff}} = 6.5/\kappa(11)$.

The product $B = \kappa L_{\text{eff}}$ is not very sensitive to the precise value of η_{10} ($B = 1.4$ for $\eta_{10} = 0.23$ and 1.5 for $\eta_{10} = 0.26$) while B is quite sensitive to η_{11} ($B = 6.5$ for $\eta_{11} = 0.69 = 3 \times 0.23$ and 17 for $\eta_{11} = 0.78 = 3 \times 0.26$). This high sensitivity of B to η_{11} is due to the fact that η_{11} is approaching 1 at the melting and in the liquid. Nevertheless this high sensitivity cannot be easily used. This simple relation between η_{Q_B} and the peak width is questionable for η_{Q_B} approaching 1 and for low value of the coherence length since the approximations used in our previous paper are no longer valid.

Figure 9 shows the variation of the coherence length with temperature, determined using the (10) peak width. It is an effective coherence length since it takes into account the finite transfer length, *i.e.*, the finite resolution. In order to have access to the real coherence length of the liquid, it would be necessary to deconvolute or to improve resolution. But, as we shall see, one must take into account the effective coherence length when analysing the intensity variation.

5.4. INTENSITY. — The quasi-long-range order not only affects the peak widths but also their intensities. Following Aranda *et al.* [20], for a powder experiment the intensity should vary as $(AL_{\text{eff}})^{1-\eta_{Q_B}}$. In the solid regime, η_{Q_B} varies and L_{eff}, being the inverse of the peak HWHM at low temperature, is constant; this effective coherence length accounts for both the finite size effect and the finite resolution effect. In the liquid regime, η_{Q_B} is constant and equal to $\eta^*_{Q_B}$, its value at the melting, and L_{eff}, being the effective coherence length determined in 5.3, varies.

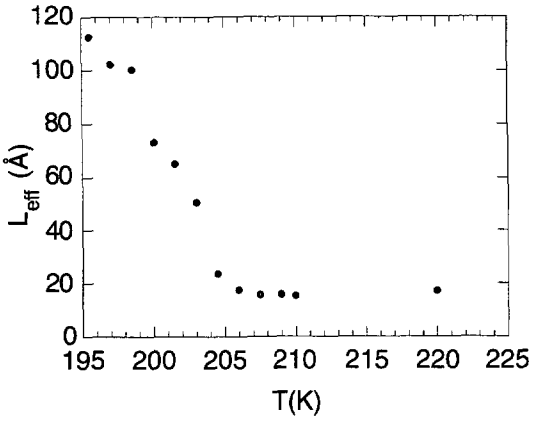

Fig. 9. — Effective length (•) *vs.* temperature.

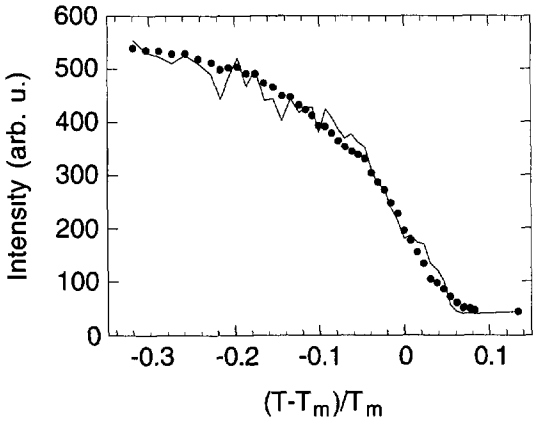

Fig. 10. — Measured intensity at the maximum of the (10) peak (●) and calculated intensity (—) *vs.* the reduced temperature (T_m is the melting temperature).

Analysing the (10) peak data, we calculated the intensity for both the regimes with the same prefactor value. As shown in Figure 10, there is a quite good agreement between the measured and calculated intensities for the two regimes. We consider the agreement between calculated and measured intensities on both sides of the transition as a very strong support for a KTHNY transition. Moreover this agreement is satisfactory down to coherence lengths as low as 30 Å, which is a surprisingly low value; this fact has already been noticed by Heiney *et al.* and Nielsen *et al.*

In Figure 11 we compare the calculated intensity with the same prefactor to the measured intensity of the (11) peak in the solid regime. There is an excellent agreement up to $\eta_{11} = 0.2$. But we have no explanation for the sudden rupture of the slope occurring for higher η_{11} values.

It is not uninteresting to discuss the value of the prefactor. The prefactor value A was determined by a least-squares fit in the solid regime and was found to be 6.2 $Å^{-1}$, whereas, in a simple model [20,22], its "theoretical" value should be $A_0 = 0.45 Q_B(10) = 0.54$ $Å^{-1}$. For a two-dimensional harmonic crystal, we have $u^2(R) = \langle |U(0) - U(R)|^2 \rangle = \ln(RA_0)\eta_{Q_B}/Q_B^2$. To

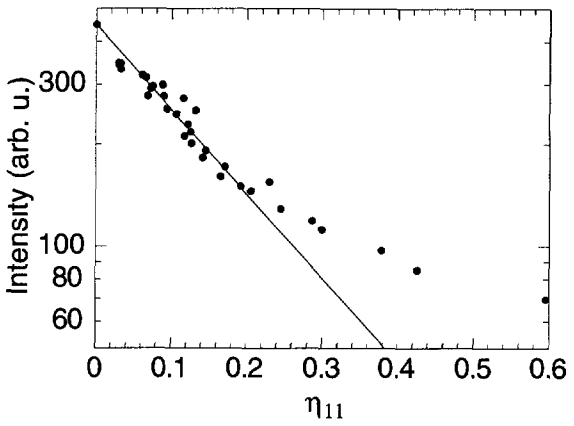

Fig. 11. — Measured intensity at the maximum of the (11) peak (●) and calculated intensity (—) *vs.* η_{11}.

account for the prefactor A, we must add to $u^2(R)$ a term $v^2 = \ln(A/A_0)\eta_{Q_B}/Q_B^2$ independent of R. We must note that v^2 is equal to 0.41 Å^2 at the melting which is lower than $u^2(R) = 1.26$ Å^2 for the farthest atoms at the same temperature. This term, v^2, which is similar to that found in a Debye-Waller calculation for a three-dimensional lattice should appear during the calculation of an optical branch contribution; but we do not understand why an optical branch should be renormalised during the melting process, as the η_{Q_B} dependence of v^2 seems to indicate.

6. Conclusion

The simultaneous observation of two diffraction peaks and the utilisation of a method allowing the measure of the parameter which controls the broadening of the peaks, lead to the following results:

- The melting of CCl_4 adsorbed on graphite is not first order but continuous.
- In the solid, the simple law $\eta_{11} = 3\eta_{10}$ is fairly verified up to $\eta_{10} = 0.23$, the value of η_{10} at melting. This relation is a test of the quasi-long-range nature of the order. The monotonous growth of η_{10} with temperature is increased when approaching 194 K, the melting temperature, providing evidence for the renormalisation of elastic constants.
- In both the solid and the liquid, the $(AL)^{1-\eta_{Q_B}}$ behaviour of the (10) peak intensity is verified using the same single free parameter A for the two phases. This verification required a correct measure of the coherence length in the liquid. Surprisingly, this power law behaviour is valid for coherence lengths as low as 30 Å. This fact, which was previously noticed by other authors, legitimates *a posteriori* the use of a substrate with crystallites of 350 Å size.

The observation of two diffraction peaks allows the study of the order in the solid and in the liquid regardless of the crystallites size. The nature of the order in the two phases, the value of η_{10} at melting and the rapid increase of η_{10} and η_{11} when approaching melting from below are in very good agreement with the Kosterlitz-Thouless-Halperin-Nelson-Young melting mechanism. Yet, it is clear that large size crystallites are needed to study the divergence of the liquid coherence length when approaching melting temperature from above. The poor quality

of our Papyex sample prevents us from doing such a study and testing the critical behaviour proposed by KTHNY theory.

Finally, the prefactor A in the intensity behaviour does not agree with the theoretical prediction. It would be worthwhile to study if this discrepancy is to be assigned to the CCl_4-on-graphite system, or is universal.

Acknowledgments

The authors are grateful to C. Aslangul, C. Marti and C. Simon for stimulating discussions and to J. I. Collar for careful reading of the manuscript.

References

[1] Abdelmoula M., Ceva T., Croset B. and Dupont-Pavlovsky N., *Surf. Sci.* **274** (1992) 129.
[2] Stephens P.W. and Huth M.F., *Phys. Rev. B* **32** (1985) 1661.
[3] Heiney P.A., Stephens P.W., Birgeneau R.J., Horn P.M. and Moncton D.E., *Phys. Rev. B* **28** (1983) 6416.
[4] Nielsen M., Als-Nielsen J., Bohr J., McTague J.P., Moncton D.E. and Stephens P.W., *Phys. Rev. B* **35** (1987) 1419.
[5] Kosterlitz J.M. and Thouless D.J., *J. Phys. C* **6** (1973) 1181.
[6] Nelson D.R. and Halperin B.I., *Phys. Rev. B* **19** (1979) 2457.
[7] Young A.P., *Phys. Rev. B* **19** (1979) 1855.
[8] Strandburg K.J., *Rev. Mod. Phys.* **60** (1988) 161 and references therein.
[9] Mehrotra R., Guenin B.M. and Dahm A.J., *Phys. Rev. Lett.* **48** (1982) 641.
[10] Guo C.J., Mast D.B., Mehrotra R., Ruan Y.-Z., Stan M.A. and Dahm A.J., *Phys. Rev. Lett.* **51** (1983) 1461.
[11] Specht E.D., Sutton M., Birgeneau R.J., Moncton D.E. and Horn P.M., *Phys. Rev. B* **30** (1984) 1589.
[12] Ecke R.E. and Dash J.G., *Phys. Rev. B* **28** (1983) 3738.
[13] Kim H.K., Zhang Q.M. and Chan M.H.W., *Phys. Rev. Lett.* **56** (1986) 1579.
[14] Murray C.A. and Van Winkle D.H., *Phys. Rev. Lett.* **58** (1987) 1200.
[15] Saito Y. and Muller-Krumbhaar H., in Applications of the Monte Carlo Method in Statistical Physics, Topics in Current Physics, Vol. 36, K. Binder Ed. (Springer, New-York, 1984) p. 223.
[16] Fernandez J.F., Ferreira M.F. and Stankiewicz J., *Phys. Rev. B* **34** (1986) 292.
[17] Strandburg K.J., *Phys. Rev. B* **35** (1987) 7161.
[18] Nuttall W.J., Noh D.Y., Wells B.O. and Birgeneau R.J., *Surf. Sci.* **307-309** (1994) 768.
[19] Abdelmoula M., Thèse, Nancy I (1991).
[20] Aranda P. and Croset B., *J. Phys. I France* **5** (1995) 1213.
[21] Warren B.E., *Phys. Rev.* **59** (1941) 693.
[22] Dutta P. and Sinha S.K., *Phys. Rev. Lett.* **47** (1981) 50.
[23] Dimon P., Horn P.M., Sutton M., Birgeneau R.J. and Moncton D.E., *Phys. Rev. B* **31** (1985) 437.